

REMOTE SENSING IN THE ANALYSIS AND CHARACTERIZATION OF SPATIAL VARIABILITY OF THE TERRITORY. A STUDY CASE IN TIMIS COUNTY, ROMANIA

Cosmin Alin POPESCU¹, Mihai Valentin HERBEI¹, Florin SALA²

¹Banat University of Agricultural Sciences and Veterinary Medicine "King Michael I of Romania" from Timisoara, Remote Sensing and GIS, Timișoara, 300645, Romania; Emails: cosmin_popescu@usab-tm.ro; mihai_herbei@yahoo.com

²Banat University of Agricultural Sciences and Veterinary Medicine "King Michael I of Romania" from Timisoara, Soil Science and Plant Nutrition, Timișoara, 300645, Romania; Email: florin_sala@usab-tm.ro

Corresponding author: florin_sala@usab-tm.ro

Abstract

The present study used satellite images analysis to evaluation and characterization of land spatial variability in the Livezile-Dolat Protected Area, Timis County, Romania. Based on the spectral information, the indices NDVI, SAVI, NBR, GLI, GNDVI and CIGreen were calculated. On the basis of ISODATA algorithm, an unsupervised analysis was performed, and 15 classes resulted. The coefficient of variation (CV) expressed a high variability in terms of the surfaces size on the set of 15 obtained classes ($CV_{Class}=43.2658$). Based on the NDVI index, 8 groups of values were obtained, covering an area of 6,542.801 ha; 9 groups of values covering the surface of 6,555.21 ha in the case of SAVI, and 6 groups of values covering the area of 6,542.955 ha in the case of CIGreen were obtained. Data series for each index studied (654,361 values per series) were analyzed to evaluate the variance (V) and coefficient of variation (CV). The highest value of the variance was identified for the CIGreen index ($V_{CIGreen}=0.892885$), and the lowest at the GLI index ($V_{GLI}=0.001912$), the other indices having intermediate values of the variance ($V_{GNDVI}=0.013837$, $V_{NDVI}=0.028027$, $V_{SAVI}=0.063048$). Based on the values of the coefficient of variation (CV), a high degree of spatial variability was found in the set of GLI index values ($CV_{GLI}=80.40968$) and the lowest spatial variability in the GNDVI index data set ($CV_{GNDVI}=23.85455$), and intermediate values for the other studied indices ($CV_{NDVI}=28.76762$, $CV_{SAVI}=28.76861$, $CV_{CIGreen}=57.57606$).

Key words: ISODATA, spatial variability, unsupervised classification, variation coefficient

INTRODUCTION

Terrestrial areas, by their specificity and complexity, have a high diversity and are studied at different levels of understanding, in relation to the issues addressed; from the global, national, regional level, to the level of administrative units, vegetative associations, farm, crop plot, or even soil unit, respectively agrochemical plot [15], [3], [25], [62], [60].

The functionality of the natural ecosystems, the productivity and the performance of the agricultural ecosystems, are permanently studied in relation to the type of ecosystem (natural or anthropic), the level of technology, the factors of production, pedo climatic

conditions, products specificity, the retail market etc. [8], [9], [50], [46], [42], [43], [45]. The facilities offered by "digitalization" are considered to have a very high potential for the optimization of agricultural production processes, technologies innovation, as management support decision in farm or environmental management [11]. Imaging analysis is increasingly present in studies, researches and evaluations of natural or agricultural ecosystems, as a result of the facilities and advantages it offers [67], [18], [19], [29], [23], [64].

In relation to the scale at which the analysis is performed, satellite images (Landsat, Sentinel 2, MODIS etc.), aerial images (utility aircraft,

UAV), or real-time terrestrial images taken with high resolution cameras, fixed on different agricultural machines are used [12], [54], [70], [65]. Spectral cameras have evolved a lot, so the captured images are at high resolutions and more and more accurately capture the realities at the plant level, agricultural crops, or natural ecosystems [36], [56], [71].

In relation to the objectives pursued, the digitization and image analysis addressed topics at foliar level [10], [53], at plant level and plant communities [40], [49], at agricultural field level [41], [58]. Digitization is very useful for the analysis and decision-making process in order to optimize the production process and can integrate and capitalize very efficiently various models and scenarios from experimental studies [51], [52].

Imaging analysis has found utility for floristic composition study, land classification and crop identification [24], [68], [39], plant health study [44], evaluation the plants response to stress factors [69], [32], [28], study of weed presence [63], [57], crop

growth dynamics evaluation [17], chlorophyll content measure [6], [7], physiological processes evaluation [26], estimation of biomass production [5], [20], or the study of rural or urban anthropic areas [37], [38].

Diversity and spatial variability of the land and the vegetal cover are faithfully reflected in the variation of the specific indices, which capture and quantify the level of heterogeneity of the studied area [59], [34], [2].

The present study used the imaging analysis based on the satellite images, for the analysis and characterization of a territory under the aspect of spatial variability in the area of Livezile-Dolat, Timis County, Romania.

MATERIALS AND METHODS

The aim of the study was to analyze and characterize the spatial variability of a territory, based on satellite images, in the Sentinel 2 satellite system, a territory that includes a complex, agricultural, anthropic and natural territory, in the context of a protected natural area, Fig. 1.

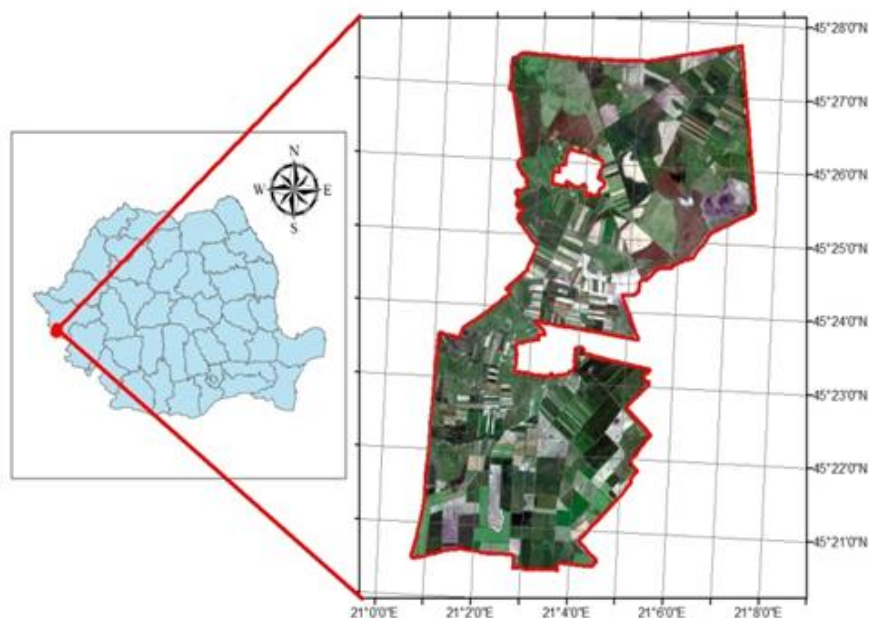


Fig. 1. Studied territory, Protected Natural Area Livezile-Dolat, Timis County, Romania

Source: original map, generated with ArcGIS based on Sentinel 2 spectral data package [55].

Study area is located in the South West part of Timiș County, Romania and is characterized by a high degree of complexity, given by

agricultural, anthropic and natural areas within the Natural Protected Area Livezile-Dolat (Directive 2009/147/EC of the

European Parliament and of the Council of 30 November 2009 on the conservation of wild birds - Birds Directive, Category of Special Bird Protection Area, code ROSPA0126).

From an administrative point of view, the Livezile-Dolat studied area is included in the 5 West Development Region, entirely on the territory of Timiș County, respectively variable distributed on the territory of five territorial administrative units: Livezile (65%), Ghilad (26%), Banloc (9 %), respectively Giera (<1%). The total area of the Livezile-Donat area is 6,565.00 ha [35], Fig. 1.

In this study, the Sentinel 2 remote sensing system was used, more precisely a scene taken on the date of 27.05.2018. Sentinel 2 represents the European Earth Observation Space mission that debuted in 2015. Sentinel 2 satellites are positioned on a solar synchronous orbit at an altitude of 786 km and take images on 13 spectral bands, of which 5 in near infrared, at 10, 20 and 60 m spatial resolution, 10 days temporal resolution, and 12 bit radiometric resolution. The data format provided was jp2 and xml, and the footprint of the images is 290 x 290 km [55].

The experimental data in the form of spectral information in the Red, Green, Blue, NIR bands were initially analyzed and processed to determine specific indices (NDVI, SAVI, NBR, GLI, GNDVI, and CIgreen). An unsupervised classification of digital images and territory was made. The type of distribution of the values of the studied indices, descriptive statistical parameters, correlation level, coefficient of variation, and variance were analyzed.

ERDAS Ymage, and ArcGIS v.10.6 softwares was used for the analysis and processing of satellite images, and for the processing of experimental data, the PAST software [16] and STATISTICA were used.

RESULTS AND DISCUSSIONS

In the analysis of digital images, unsupervised classification implies the generation of pixel groups with specific geographical

representation, but without knowing the reality that they classify. After the unsupervised classification obtained, the significance of the pixels in the analyzed digital image, expressed in the classes generated, is verified and confirmed with the reality in the field.

The unsupervised classification is based on mathematical algorithms such as ISODATA (Iterative Self Organizing Data Analysis) and K-Means, and in the present study the classification was made based on the ISODATA algorithm [4]. The ISODATA algorithm for images analysis and classification is based on determining the minimum spectral distance for cluster formation, based on the affinity of the spectral information.

The analysis and classification equation based on the spectral distances, is actually based on the equation used to determine the Euclidean distances, relation (1), [61], [33], [1].

$$SD_{xyc} = \sqrt{\sum_{i=1}^n (\mu_{ci} - X_{xyi})^2} \quad (1)$$

where: n - number of bands; i - band number; c - particular class; X_{xyi} - data file value of pixel x, y in band i ; μ_{ci} - mean of data file values (digital numbers) in band i for the sample the class c ; SD_{xyc} - spectral distance from pixels x, y to the mean of class c

Of the 13 spectral bands provided by Sentinel 2, in the present study for natural color imaging - RGB, spectral bands 4 (Red), 3 (Green) and 2 (Blue) were used, which have a spatial resolution of 10 m.

For false color image (NIR-Red-Green) spectral bands 8 (Nir), 4 (Red), and 3 (Green) were used. This image was subjected to an unsupervised classification, resulting in a number of 15 classes, with the configuration presented in table 1. The spatial distribution of the classes determined in the study area is presented in Fig. 2.

Based on the spectral bands 8 (NIR1), 8a (NIR5), 12 (SWIR2), 4 (RED), 3 (GREEN, and 2 (BLUE), 6 indices were calculated for the characterization of the studied area.

The Normalized Difference Vegetation Index

(NDVI) [47], [48], [66] was calculated based on relation (2).

$$NDVI = \frac{NIR - RED}{NIR + RED} = \frac{BAND8 - BAND4}{BAND8 + BAND4} \quad (2)$$

Table 1. The structure by classes and surfaces resulting from the unsupervised classification of the studied area (Protected Natural Area Livezile-Dolat, Timis County, Romania)

Class	Sum of Arias	Percent
1	213.33	3.25
2	406.75	6.20
3	316.41	4.83
4	425.56	6.49
5	261.84	3.99
6	406.94	6.21
7	500.98	7.64
8	557.36	8.50
9	730.11	11.13
10	287.34	4.38
11	794.57	12.12
12	451.18	6.88
13	661.04	10.08
14	420.13	6.41
15	123.66	1.89
Total	6,557.2	100

Source: original data, resulted by unsupervised classification of false color image generated by ArcGIS.

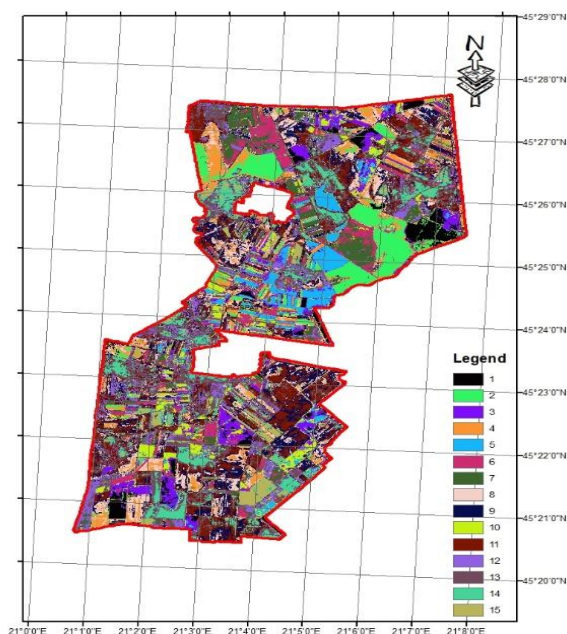


Fig. 2. Unsupervised classification of the studied area (Protected Natural Area Livezile-Dolat, Timis County, Romania)

Source: original map, generated based on false color image; Sentinel 2 spectral data package [55], ArcGIS software.

The range of variation of the NDVI values, and the corresponding surfaces, are presented in table 2. Based on the NDVI index, an area of 6,542.801 ha was covered, compared to the total area of 6,565.00 ha, which represents 99.66%. NDVI variation range, in relation to pixels number for studied area is presented in Fig. 3. The graphical representation of the NDVI index for the studied area, in the form of map, is presented in Fig. 4.

Table 2. Range of variation and related area in case of NDVI index for the studied area (Protected Natural Area Livezile-Dolat, Timis County, Romania)

Group	Range of variation	Area	%
1	-0.054886- 0.229541	314.7178	4.81
2	0.229541 – 0.306792	349.843	5.35
3	0.306792 – 0.384044	376.63	5.76
4	0.384044 – 0.457784	467.1389	7.14
5	0.457784 – 0.531524	585.3623	8.95
6	0.531524 – 0.605265	704.0567	10.76
7	0.605265 – 0.671982	1,015.168	15.51
8	0.671982 – 0.724653	1,366.179	20.88
9	0.724653 – 0.844042	1,363.706	20.84
Total		6,542.801	100.00

Source: original data, obtained by NDVI values analysis.

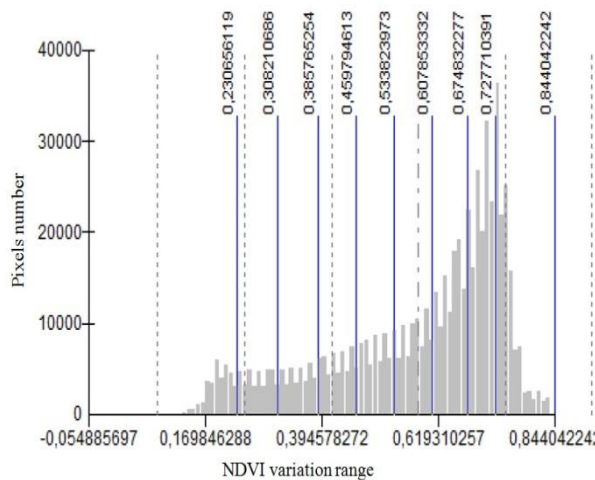


Fig. 3. NDVI variation range in relation to pixels number for studied area

Source: original graph, generated based on NDVI values, ArcGIS software.

The Normalized Burn Ratio index (NBR) was determined according to the relation (3), [27]. Graphical distribution of NBR index values for the studied area, in the form of map, is presented in Fig. 5.

$$NBR = \frac{NIR - SWIR}{NIR + SWIR} = \frac{BAND8a - BAND12}{BAND8a + BAND12} \quad (3)$$

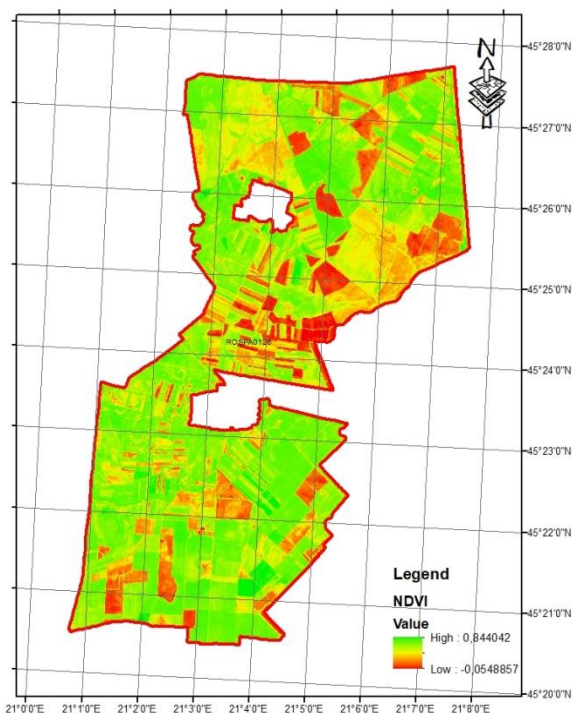


Fig. 4. Map with the spatial distribution of NDVI index values

Source: original map, generated based on NDVI values, ArcGIS software.

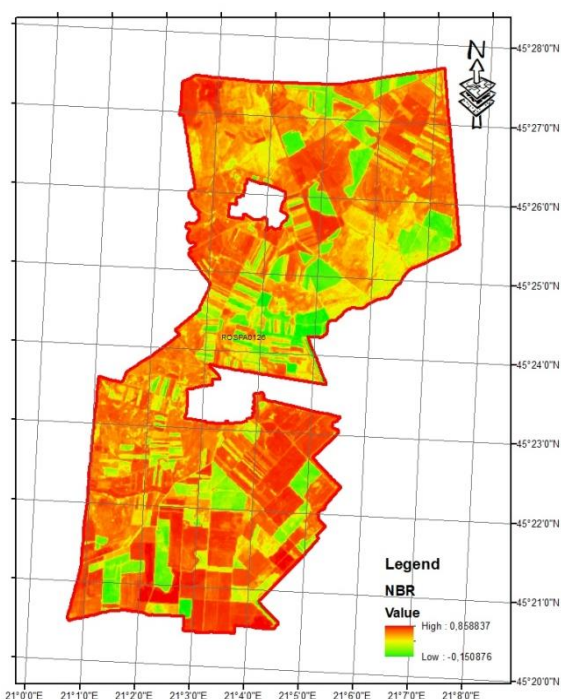


Fig. 5. Map with the spatial distribution of NBR index values

Source: original map, generated based on NBR values, ArcGIS software.

SAVI (Soil Adjusted Vegetation Index), relation (4), was proposed and developed as a modification of the vegetation index [21],

with differences normalized in order to correct the influence of the soil luminosity in the conditions in which the vegetation land cover is low.

$$SAVI = \frac{NIR - RED}{NIR + RED + L}(1 + L) = \frac{BAND\ 8 - BAND\ 4}{BAND\ 8 + BAND\ 4}(1 + L) ;$$

$$L = 0.5 \quad (4)$$

The range of variation of the SAVI values and the corresponding surfaces are presented in table 3. SAVI variation range in relation to pixels number for studied area is presented in Fig. 6.

Table 3. The range of variation and the related area in the case of the SAVI index for the studied area

Group	Range of variation	Area	%
1	-0.082325 – 0.344284	315.31	4.81
2	0.344284 – 0.460152	350.23	5.34
3	0.460152 – 0.576021	377.76	5.76
4	0.576021 – 0.686623	468.19	7.14
5	0.686623 – 0.797226	586.54	8.95
6	0.797226 – 0.907828	706.21	10.77
7	0.907828 – 1.007896	1,017.4	15.52
8	1.007896 – 1.086898	1,368.92	20.88
9	1.086898 – 1.265968	1,364.65	20.82
Total		6,555.21	100

Source: original data, obtained by SAVI values analysis.

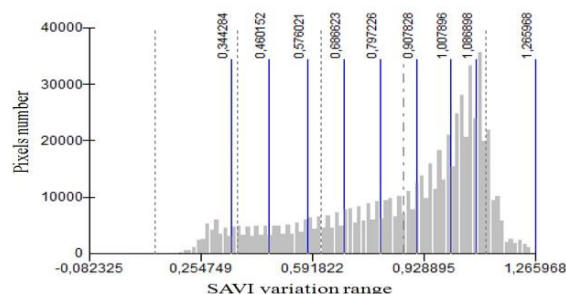


Fig. 6. SAVI variation range in relation to pixels number for studied area

Source: original graph, generated based on NBR values, ArcGIS software.

Based on the SAVI index, an area of 6,555.21 ha was covered, compared to the total area of 6,565.00 ha, which represents 99.81%. The numerical values and the graphical distribution of the SAVI index express with high accuracy the situation in the studied area, in a variation interval between -0.082325 and 1.265968. Graphical distribution of the SAVI index values for the studied area, in the form of map, is presented in Fig. 7.

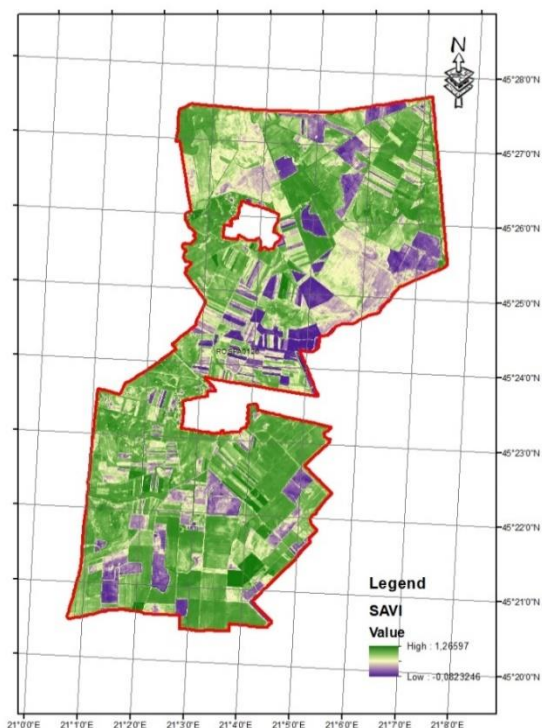


Fig. 7. Map with the spatial distribution of SAVI index values
 Source: original map, generated based on SAVI values, ArcGIS software.

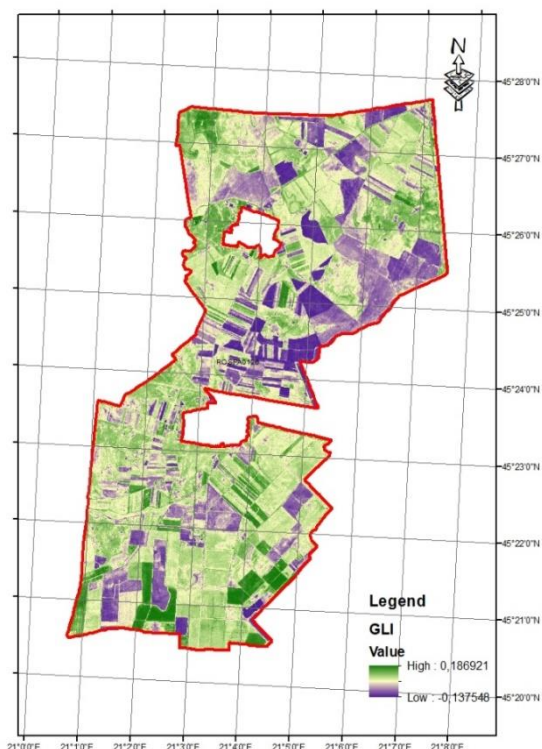


Fig. 8. Map with the spatial distribution of GLI index values
 Source: original map, generated based on GLI index values, ArcGIS software.

Green Leaf Index (GLI), was determined based on the relation (5), [31], [22]. GLI values range from -1 to +1. The negative values represent the soil and the "non-living features" of the soil, while the positive values represent the leaves and the green stems. Graphical distribution of the GLI index values for the studied area, in the form of map, is presented in Fig. 8.

$$GLI = \frac{2 \cdot GREEN - RED - BLUE}{2 \cdot GREEN + RED + BLUE} = \frac{2 \cdot BAND\ 3 - BAND\ 4 - BAND\ 2}{2 \cdot BAND\ 3 + BAND\ 4 + BAND\ 2} \quad (5)$$

Green NDVI, relation (6), [13], [30], is similar to NDVI, except that it measures the green spectrum from 540 to 570 nm instead of the red spectrum. This index is more sensitive to chlorophyll concentration than NDVI.

$$GNDVI = \frac{NIR - GREEN}{NIR + GREEN} = \frac{BAND\ 8 - BAND\ 3}{BAND\ 8 + BAND\ 3} \quad (6)$$

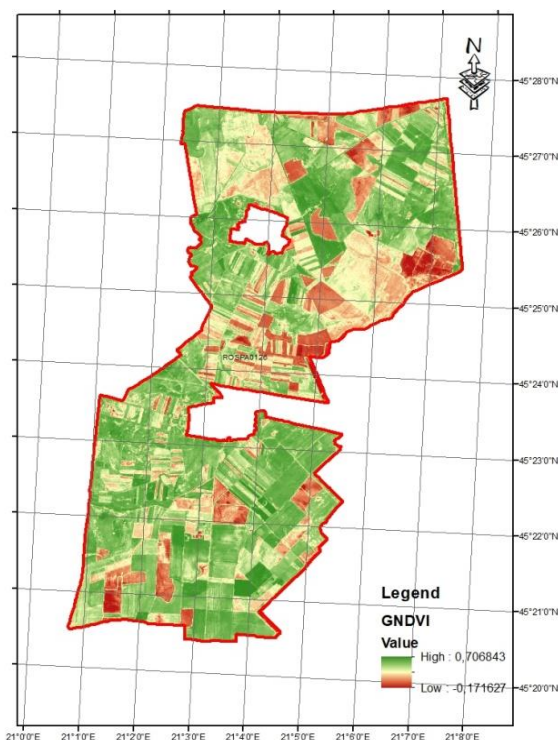


Fig. 9. Map with the spatial distribution of GNDVI index values
 Source: original map, generated based on GNDVI index values, ArcGIS Software.

GNDVI uses the green band in the visible spectrum (instead of red as in the NDVI) and

the NIR band. The use of green band is useful for measuring photosynthesis rates and monitoring plant stress. The graphical distribution of the GNDVI index for the studied area, in the form of map, is presented in Fig. 9.

Chlorophyll index green (CIgreen), relation (7), [14], [22], was used to estimate the chlorophyll content of leaves, in a wide range of plant species.

$$CI_{green} = \frac{NIR}{GREEN} - 1 = \frac{BAND\ 8}{BAND\ 3} - 1 \quad (7)$$

The CIgreen marginal values are sensitive to small variations in chlorophyll content and are consistent with most species. The range of variation of CIgreen values and the corresponding area are presented in Table 4.

Table 4. The range of variation and the related area in the case of the CIgreen index for the studied area

Group	Values	Area (ha)	Percentage
1	-1	0.02	0.0003
2	0.99 - 0	805.2145	12.3066
3	0.001-1	2,023.497	30.9264
4	1.01-2	0.00	0.00
5	2.01-3	2,491.385	38.0774
6	3.01-4	1,222.839	18.6894
Total		6,542.955	100.00

Source: original data, resulted by CIgreen values analysis.

CIgreen variation range in relation to pixels number for studied area is presented in fig. 10. Based on the CIgreen index, an area of 6,542.955 ha was covered, compared to the total area of 6,565.00 ha, which represents 99.66%. Graphical distribution of the CIgreen index values for the studied area, in the form of map, is presented in Fig. 11.

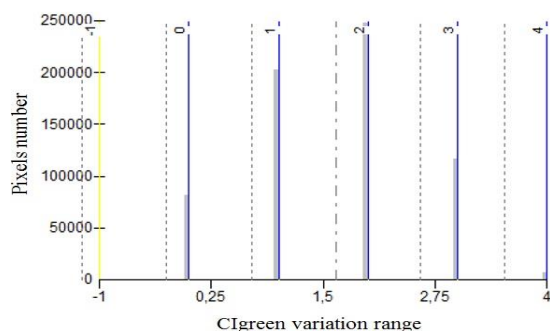


Fig. 10. CIgreen variation range in relation to pixels number

Source: original graph, generated based on CIgreen values, ArcGIS Software.

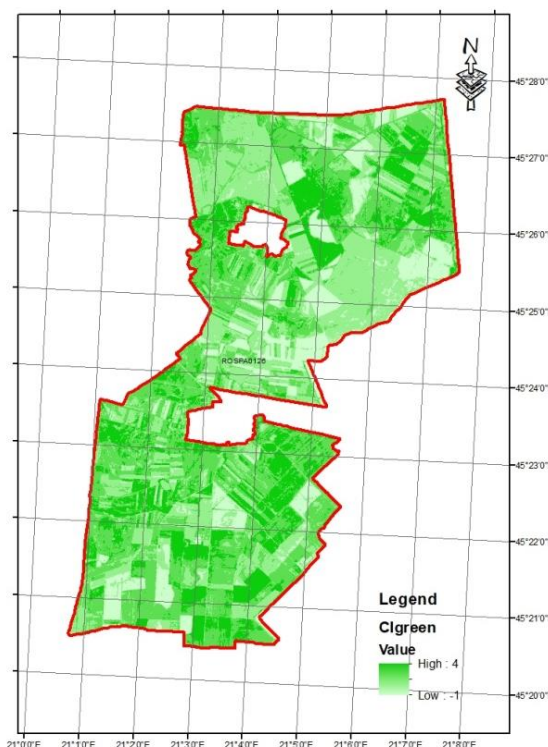


Fig. 11. Map with the spatial distribution of CIgreen index values

Source: original map, generated based on CIgreen index values, ArcGIS Software.

Descriptive statistical analysis of the experimental data set for the indices used in the analysis and classification of the studied area (a total number of 654,361 data), led to the values presented in Table 5. From the analysis of the respective data, a high variance of the CIgreen index was found, and the coefficient of variation highlighted the highest value of the GLI index. The correlation analysis led to the data in table 6, and showed the existence of very high positive correlations between most indices, high correlation between GLI and GNDVI, respectively a medium level correlation between GLI and CIgreen.

Table 5. Statistical parameters of the values of the studied indices

	NDVI	SAVI	CIgreen	GNDVI	GLI
N	654,361	654,361	654,361	654,361	654,361
Min	-0.05489	-0.08232	-1	-0.17163	-0.13755
Max	0.844042	1.26597	4	0.706843	0.186921
Mean	0.581945	0.872804	1.641178	0.493111	0.054374
Std. error	0.000207	0.00031	0.001168	0.000145	5.40E-05
Variance	0.028027	0.063048	0.892885	0.013837	0.001912
Coeff. var	28.76762	28.76861	57.57606	23.85455	80.40968

Source: original data, resulted from studied indices analysis.

Table 6. Correlation table between the values of the studied indices

	NDVI	SAVI	Cigreen	GNDVI	GLI
NDVI					
SAVI	0.999				
Cigreen	0.907	0.907			
GNDVI	0.982	0.982	0.933		
GLI	0.903	0.903	0.771	0.847	

Source: original data, resulted from studied indices analysis.

CONCLUSIONS

The unsupervised classification, based on the ISODATA algorithm, of a false color image (NIR-Red-Green), spectral bands 8 (Nir), 4 (Red), and 3 (Green) resulted in 15 classes representing 6,557.2 ha from study area. Calculated indices (NDVI, SAVI, NBR, GLI, GNDVI, Cigreen) based on spectral data, bands 8 (NIR1), 8a (NIR5), 12 (SWIR2) and 4 (RED), 3 (GREEN), 2 (BLUE) facilitated characterization of the territory, and they have faithfully surprised the spatial variability of the studied area. A high degree of spatial variability was found in the set of GLI index values ($CV_{GLI} = 80.40968$) and the lowest spatial variability in the GNDVI index data set ($CV_{GNDVI} = 23.85455$).

ACKNOWLEDGMENTS

The authors thanks to the GEOMATICS Research Laboratory, BUASMV "King Michael I of Romania" from Timisoara, for the facility of the software use for this study.

REFERENCES

[1]Abbas, A.W., Minallh, N., Ahmad, N., Abid, S.A.R., Khan, M.A.A., 2016, K-Means and ISODATA clustering algorithms for landcover classification using remote sensing, Sindh Univ. Res. Jour. (Sci. Ser.), 48(2):315-318.
 [2]Ali, A., Martelli, R., Lupia, F., Barbanti, L., 2019, Assessing multiple years' spatial variability of crop yields using satellite vegetation indices, Remote Sens., 11(20):2384.
 [3]Antle, J.M., Jones, J.W., Rosenzweig, C., 2017, Next generation agricultural system models and knowledge products: Synthesis and strategy, Agric. Syst., 155:179-185.
 [4]Ball, H.G., Hall, D.J., 1965, ISODATA, a novel

method of data analysis and pattern classification, Stanford Research Institute Menlo Park, California, Technical Report April 1965, for Information Sciences ranch Office of Naval Research Contract Nonr 4918(00) SRI Project 5533.

[5]Bendig, J., Bolten, A., Bennertz, S., Broscheit, J., Eichfuss, S., Bareth, G., 2014, Estimating biomass of barley using crop surface models (CSMs) derived from UAV-based RGB imaging, Remote Sens., 6(2014): 10395-10412.

[6]Carmona, F., Rivas, R., Fonnegra, D.C., 2015, Vegetation Index to estimate chlorophyll content from multispectral remote sensing data, Eur. J. Remote Sens., 48:319-326.

[7]Croft, H., Arabian, J., Chen, J.M., Shang, J., Liu, J., 2019, Mapping within-field leaf chlorophyll content in agricultural crops for nitrogen management using Landsat-8 imagery, Precis. Agric., 2019:1-25.

[8]Dobrei, A., Poiana, M.A., Sala, F., Ghita, A., Gergen, I., 2010, Changes in the chromatic properties of red vines from *Vitis vinifera* L. cv. Merlot and Pinot Noir during the course of aging in bottle, J. Food, Agri. Environ., 8(2): 20-24.

[9]Dobrei, A., Dobrei, A.G., Nistor, E., Iordanescu, O.A., Sala, F., 2015, Local grapevine germplasm from Western of Romania - An alternative to climate change and source of typicity and authenticity, Agric. Agric. Sci. Procedia, 6:124-131.

[10]Drienovsky, R., Nicolin, A.L., Rujescu, C., Sala, F., 2017, Scan LeafArea – A software application used in the determination of the foliar surface of plants, Res. J. Agric. Sci., 49(4):215-224.

[11]Fielke, S., Taylor, B., Jakku, E., 2020, Digitalisation of agricultural knowledge and advice networks: A state-of-the-art review, Agric. Syst., 180:102763.

[12]Fonji, S.F., Taff, G.N., 2014, Using satellite data to monitor land-use land-cover change in North-eastern Latvia. SpringerPlus, 3:61.

[13]Gitelson, A., Kaufman, Y., Merzlyak, M., 1996, Use of a green channel in remote sensing of global vegetation from EOS-MODIS, Remote Sens. Environ., 58(3):289-298.

[14]Gitelson, A.A., Viña, A., Arkebauer, T.J., Rundquist, D., Keydan, G., Leavitt, B., 2003, Remote estimation of leaf area index and green leaf biomass in maize canopies, Geophys. Res. Lett., 30(5):52-1-52-4.

[15]Govedarica, M., Ristic, A., Herbei M.V., Sala, F., 2015, Object oriented image analysis in remote sensing of forest and vineyard areas, BulletinUASVM Horticulture 72(2):362-370.

[16]Hammer, Ø., Harper, D.A.T., Ryan, P.D., 2001, PAST: Paleontological statistics software package for education and data analysis, Palaeontol. Electron., 4(1):1-9.

[17]Herbei, M.V., Sala, F., 2015, Use Landsat image to evaluate vegetation stage in sunflower crops. AgroLife Sci. J., 4(1):79-86.

[18]Herbei, M., Sala, F., Boldea, M., 2015a, Relation of Normalized Difference Vegetation Index with some spectral bands of satellite images. AIP Conf. Proc.,

1648:670003-1 – 670003-4.

- [19]Herbei, M., Sala, F., Boldea, M., 2015b, Using mathematical algorithms for classification of Landsat 8 satellite images. AIP Conf. Proc., 1648:670004-1 – 670004-4.
- [20]Herbei, M., Sala, F., 2016, Biomass prediction model in maize based on satellite images. AIP Conf. Proc., 1738:350009-1 – 350009-4.
- [21]Huete, A.R., 1988, A Soil-Adjusted Vegetation Index (SAVI), Remote Sens. Environ., 25(3):295-309.
- [22]Hunt, E.R., Daughtry, C.S.T., Eitel, J.U.H., Long, D.S., 2011, Remote sensing leaf chlorophyll content using a visible band index, Agron. J., 103(4):1090-1099.
- [23]Iagăru, P., Pavel, P., Iagăru, R., 2019, Implementation of the concept agriculture of precision a way to improve the management of agricultural enterprises, Scientific Papers Series Management, Economic Engineering in Agriculture and Rural Development, 19(1): 229-234.
- [24]Kalaba, F.K., Quinn, C.H., Dougill, A.J., Vinya, R., 2013, Floristic composition, species diversity and carbon storage in charcoal and agriculture fallows and management implications in Miombo woodlands of Zambia, For. Ecol. Manag., 304:99-109.
- [25]Kalaugher, E., Beukes, P., Bornman, J.F., Clark, A., Campbell, D.I., 2017, Modelling farm-level adaptation of temperate, pasture-based dairy farms to climate change. Agric. Syst., 153:53-68.
- [26]Kasampalis, D.A., Alexandridis, T.K., Deva, C., Challinor, A., Moshou, D., Zalidis, G., 2018, Contribution of remote sensing on crop models: A review. J. Imaging, 4:52.
- [27]Key, C.H., Benson, N., Ohlen, D., Howard, S., McKinley, R., Zhu Z., 2002, The normalized burn ratio and relationships to burn severity: ecology, remote sensing and implementation, Proceedings of the Ninth Forest Service Remote Sensing Applications Conference. American Society for Photogrammetry and Remote Sensing, Bethesda, MD, J.D. Greer, ed. Rapid Delivery of Remote Sensing Products.
- [28]Khanna, R., Schmid, L., Walter, A., Nieto, J., Siegwart, R., Liebisch, F., 2019, A spatio temporal spectral framework for plant stress phenotyping, Plant Methods, 15:13.
- [29]Knicker, K., Maréchal, A., 2018, Stimulating the social and environmental benefits of agriculture and forestry: An EU-based comparative analysis, Land Use Policy, 73:320-330.
- [30]Le Maire, G., François, C., Dufrêne, E., 2004, Towards universal broad leaf chlorophyll indices using PROSPECT simulated database and hyperspectral reflectance measurements. Remote Sens. Environ. 89(1):1-28
- [31]Louhaichi, M., Borman, M., Johnson, D., 2001, Spatially located platform and aerial photography for documentation of grazing impacts on wheat. Geocarto Int., 16(1):65-70.
- [32]Lowe, A., Harrison, N., French, A.P., 2017, Hyperspectral image analysis techniques for the detection and classification of the early onset of plant disease and stress, Plant Methods, 13:80.
- [33]Melesse, A.M., Jordan, J.D., 2002, A comparison of Fuzzi vs. Augmented-ISODATA classification algorithms for cloud-shadow discrimination from Landsat images, Photogramm. Eng. Rem. S., 68(9):905-911.
- [34]Militino, A.F., Ugarte, M.D., Pérez-Goya, U., 2018, An introduction to the spatio-temporal analysis of satellite remote sensing data for geostatisticians. In: Daya Sagar B., Cheng Q., Agterberg F. (eds) Handbook of Mathematical Geosciences. Springer, Cham., 239-253.
- [35]M.M.A.P., 2016, Regulation of June 28, 2016 on Natura 2000 site ROSPA0126 Livezile-Dolaț, Official Monitor 805 bis (Regulamentul din 28 iunie 2016 sitului Natura 2000 ROSPA0126 Livezile-Dolaț, Monitorul Oficial 805 bis), 12.10.2016.
- [36]Murillo-García, F.G., Alcántara-Ayala, I., Ardizzone, F., Cardinali, M., Fiourucci, F., Guzzetti, F., 2015, Satellite stereoscopic pair images of very high resolution: A step forward for the development of landslide inventories, Landslides, 12:277-291.
- [37]Oncia, S., Herbei, M., Popescu, C. 2013a, Study of territorial and infrastructure development in the Petrosani city - The Hunedoara county using GIS elements, J. Environ. Prot. Ecol., 14(1):225-232.
- [38]Oncia, S., Herbei, M., Popescu, C., 2013b, Sustainable development of the Petrosani City, the Hunedoara County based on GIS analysis, J. Environ. Prot. Ecol., 14(3):232-240.
- [39]Pande, C.B., Moharir, K.N., Khadri, S.F.R., Patil, S., 2018, Study of land use classification in an arid region using multispectral satellite images. Appl. Water Sci., 8:123.
- [40]Paz-Kagan, T., Silver, M., Panov, N., Karnieli, A., 2019, Multispectral approach for identifying invasive plant species based on flowering phenology characteristics. Remote Sens., 11:593.
- [41]Peralta, N.R., Assefa, Y., Du, J., Barden, C.J., Ciampitti, I.A., 2016, Mid-season high-resolution satellite imagery for forecasting site-specific corn yield, Remote Sens., 8:848.
- [42]Popescu, A., 2018, Maize and wheat - top agricultural products produced, exported and imported by Romania, Scientific Papers Series Management, Economic Engineering in Agriculture and Rural Development, 18(3):339-352.
- [43]Popescu, A., Dinu, T.A., Stoian, E., 2018, Sorghum - an important cereal in the world, in the European Union and Romania, Scientific Papers Series Management, Economic Engineering in Agriculture and Rural Development, 18(4):271-284.
- [44]Prakash, K., Saravanamoothi, P., Sathishkumar, R., Parimala, M., 2017, A study of image processing in agriculture, Int. J. Adv. Netw. Appl., 9(1):3311-3315.
- [45]Prăvălie, R., Sîrodoev, I., Patriche, C., Roșca, B., Piticar, A., Bandoc, G., Sfică, L., Țișcovschi, A., Dumitrașcu, M., Chifiriuc, C., Mănoiu, V., Iordache, Ș., 2020, The impact of climate change on agricultural productivity in Romania. A country-scale assessment based on the relationship between climatic water

balance and maize yields in recent decades, *Agric. Syst.*, 179:102727.

[46]Rawashdeh, H.M., Sala, F., 2016, Effect of iron and boron foliar fertilization on yield and yield components of wheat, *Rom. Agric. Res.*, 33:241-249.

[47]Rouse, J.W.Jr., Haas, R.H., Schell, J.A., Deering, D.W., 1973a, Monitoring the vernal advancement and retrogradation (green wave effect) of natural vegetation. *Prog. Rep. RSC 1978-2*, Remote Sensing Center, Texas A&M Univ., College Station, 93p. (NTIS No. E73-106393).

[48]Rouse, J.W., Haas, R.H., Schell, J.A., Deering, D.W., 1973b, Monitoring vegetation systems in the Great Plains with ERTS, Third ERTS Symposium, NASA SP-351 I:309-317.

[49]Runnström, M.C., Ólafsdóttir, R., Blanke, J., Berlin, B., 2019, Image analysis to monitor experimental trampling and vegetation recovery in icelandic plant communities, *Environ.*, 6(9):99.

[50]Sala, F., Boldea, M., 2011, On the optimization of the doses of chemical fertilizers for crops, *AIP Conf. Proc.*, 1389:1297-1300.

[51]Sala F., Boldea, M., Rawashdeh, H., Nemet, I., 2015, Mathematical model for determining the optimal doses of mineral fertilizers for wheat crops, *Pak. J. Agric. Sci.*, 52(3):609-617.

[52]Sala, F., Rujescu, C., Constantinescu, C., 2016, Causes and solutions for the remediation of the poor allocation of P and K to wheat crops in Romania, *AgroLife Sci. J.*, 5(1):184-193.

[53]Sala, F., Iordănescu, O., Dobrei, A., 2017, Fractal analysis as a tool for pomology studies: Case study in apple, *AgroLife Sci. J.*, 7(2):224-233.

[54]Scheffield, K., Morse-McNabb, E., 2014, Using satellite imagery to asses trends in soil and crop productivity across landscapes. *IOP Conf. Series: Earth Environ. Sci.* 25(2015):012013.

[55]Sentinel-2 Missions, Sentinel online, ESA Sentinel, <https://sentinel.esa.int/web/sentinel/missions/sentinel-2>, Accessed on Sept.20, 2019.

[56]Shamshiri, R.R., Weltzien, C., Hameed, I.A., Yule, I.J., Grift, T.E., Balasundram, S.K., Pitonakova, L., Ahmad, D., Chowdhary, G., 2018, Research and development in agricultural robotics: A perspective of digital farming, *Int. J. Agric. Biol. Eng.*, 11(4):1-14.

[57]Shaw, D.R., 2005, Remote sensing and site-specific weed management, *Front. Ecol. Environ.*, 3(10):526-532.

[58]Sicre, C.M., Fieuzal, R., Baup, F., 2020, Contribution of multispectral (optical and radar) satellite images to the classification of agricultural surfaces. *Int. J. Appl. Earth Obs. Geoinf.*, 84:101972.

[59]Silveira, E.M.O., Mello, J.M., Júnior, F.W.A., Reis, A.A., Withey K.D., Ruiz, L.A., 2017, Characterizing landscape spatial heterogeneity using semivariogram parameters derived from NDVI images, *Cerne*, 23(4):413-422.

[60]Stupen, N., Stupen, M., Stupen, O., 2018, Electronic agricultural maps formation on the basis of GIS and earth remote sensing, *Scientific Papers Series Management, Economic Engineering in Agriculture*

and Rural Development, 18(4):347-352.

[61]Swain, P.H., Davis, S.M., 1978, *Remote Sensing: The Quantitative Approach*, McGraw Hill Book Company, New York, N.Y., 396 pp.

[62]Therond, O., Duru, M., Roger-Estrade, J., Richard, G., 2017, A new analytical framework of farming system and agriculture model diversities. A review, *Agron. Sustain. Dev.* 37:21.

[63]Thorp, K.R., Tian, L.F., 2004, A review on remote sensing of weeds in agriculture, *Precis. Agric.*, 5(5):477-508.

[64]Tian, H., Wang, T., Liu, Y., Qiao, X., Li, Y., 2019, Computer vision technology in agricultural automation - A review. *Inform. Process. Agric.*, in press.

[65]Todorova, L., Tcacenco, A., 2019, Study regarding peculiarities of introducing and developing effective digital technologies in the agrifood sector. *Scientific Papers Series Management, Economic Engineering in Agriculture and Rural Development*, 19(4):341-344.

[66]Tucker, C.J., 1979, Red and photographic infrared linear combinations for monitoring vegetation, *Remote Sens. Environ.*, 8(2):127-150.

[67]Vibhute, A., Bodhe, S.K., 2012, Applications of image processing in agriculture: A survey. *Int. J. Comput. Appl.*, 52(2):34-40.

[68]Vorobiova, N.S., 2016, Crops identification by using satellite images and algorithm for calculating estimates. *CEUR Workshop Proc.*, 1638:419-427.

[69]Wang, R., Cherkauer, K., Bowling, L., 2016, Corn response to climate stress detected with satellite-based NDVI time series, *Remote Sens.*, 8:269.

[70]Wolfert, S., Ge, L., Verdouw, C., Bogaardt, M.-J., 2017, Big data in smart farming - A review. *Agric. Syst.* 153:69-80.

[71]Yang, C., 2018, High resolution satellite imaging sensors for precision agriculture, *Front. Agric. Sci. Eng.*, 5(4):393-405.